STUDIES ON Mn^{2+} ION DOPED DOUBLE PEROVSKITE HALIDES FOR LIGHT EMITTING DEVICES

A SYNOPSIS

Submitted by

JEEVARAJ M

(Reg. No. 9200026001)

in partial fulfillment for the award of the degree

of

DOCTOR OF PHILOSOPHY

DEPARTMENT OF PHYSICS

SCHOOL OF ADVANCED SCIENCES

KALASALINGAM ACADEMY OF RESEARCH AND EDUCATION

(DEEMED TO BE UNIVERSITY)

ANAND NAGAR, KRISHNAN KOIL - 626 126

TAMIL NADU, INDIA

APRIL 2023

STUDIES ON Mn^{2+} ION DOPED DOUBLE PEROVSKITE HALIDES FOR LIGHT-EMITTING DEVICES

1. Introduction

Globally lighting accounts for more than 19% of world's electricity consumption in cities alone [1]. The daily rhythm of human life has changed since the invention of electric light by Edison in the year 1879. Spermicide oil lamps used in those days were able to provide light for only a meagre 7 hours while Edison's bulb provided 1200 hours of artificial illumination for the identical price. Now that lighting works 24 hours a day, 60 – 80 % of the world's energy needs accounts for the light polluting the night skies in cities. Most of these energy requirements are derived from fossil fuels which are fast depleting. Of these, oil and coal are more used for energy production. However, these sources produce carbon dioxide and have adverse effects on the environment such as global warming, pollution and climate change. Hence, there is a need to address this issue either with the use of renewable energy resources or by boosting the efficiency of the light sources. Much of the recent research focus on developing technologies that will reduce the dependence on fossil fuels to produce and store electric energy. For instance, improvements in the field of solar energy harvesting and enhancing the energy storage capacities of the batteries will be an effective way of clean and efficient way of energy generation and storage. Astonishingly, the incandescent light discovered by Edison in the 19^{th} century is still in use in spite of its poor efficiencies.

Over the years, other lighting sources such as compact fluorescent lamp (CFL) and light emitting diodes (LED) have gradually replaced the incandescent bulbs to a significant extent in view of their better efficiency and long life span. In particular, commercial LED's have an average life span of 25,000 hours which is 20 times better than the incandescent sources and can be fabricated using environmental friendly materials unlike CFL sources. Even though the CFL lights have a better efficiency rating than the incandescent lights, they use harmful mercury gas to produce ultraviolet light (UV) which excites the fluorescent coating in the inside of the glass tubing of a CFL lamp. Thus, on all fronts LED's have established themselves as the best artificial lighting sources.

Solid state LED's are made up of various semiconductor materials such as organic, inorganic and polymers which works on the principle of electron – hole recombination to produce light. Most notable white LED's these days are made of optically pumped light emitting diode (Op-LED). Op-LED's employ $Ga_{1-y}In_yN$ semiconductor which emit light in the blue region when a bias is applied. Part of this light is then absorbed by another phosphor that is coated on top of the $Ga_{1-y}In_yN$ LED, which then emits the remaining portion of the RGB (Red, Green, Blue) colors to produce white light. Apart from being efficient and long lasting, the very compact size of the Op-LED's provide them with greater vibration and shock resistance in comparison with the brittle glass bulbs and filament wires [2].

Scientists trio's, professor Isamau Akasaki, professor Hiroshi Amano and professor Shuji Nakamura in Japan and US were awarded 2014 Noble prize in Physics for inventing energy saving white light sources using blue LED's along with down conversion phosphors [3]. Such is the importance of this Op-LED's. An important part of this LED architecture is the down conversion phosphor, which is the reason behind emitting colors missing from the blue LED's. Thus, this phosphor coating has a significant effect on the quality of light being produced. The following characteristics are used to describe the performance of an LED and they are luminous efficiency, correlated color temperature (CCT) and color rendering index (CRI). CRI is defined as a light source's ability to faithfully reveal the color of an object in comparison to sunlight and it depends on the spectrum emitted by the light source. So, if a light source has a CRI close to 100, then it is considered to be a good light emitter. Similarly, warm white light preferred for residential areas require a CCT of 2700 K, while the commercially available Ce^{3+} : $Y_3Al_5O_{12}$ phosphor together with blue LED's exhibit a CRI of 80 and a CCT of 3000 K [3,4]. This low value of CRI and CCT are due to a less proportion of red light (600 nm) in this system which results in cold white light.

Therefore, the relative percentage of red emission should be increased via adding other red phosphor sources. However, traditionally considered rare earth activator incorporated inorganic phosphors such as Ce^{3+}:$Y_3Al_5O_{12}$, $Ca_5F(PO_4)_3$:Sb,Mn, $MgSi_2O_6$:Mn, ZnO:Zn, $CaMgSi_2O_6$:Ce, $Sr_6(Y_{1-x}Ce_x)_2Al_4O_{15}$ are limited by their high temperature synthesis route and also it lacks the required color purity [5,6]. On the other hand, quantum dot phosphors exhibit high color purity but their upscaling is restricted

by the agglomeration which affects it stability [7–11]. In view of this, it is necessary to develop new luminescent semiconductors that may be processed at low temperatures using low cost precursors. Semiconductors with new luminescent properties can be obtained by doping appropriate doping atoms into the semiconductor known as "activators" to design LED's with desired optical properties. The dopant can also act as a "sensitizer" as well as to absorb the incident photon energy and transfer it to the activator sites for emission. There are numerous choice of elements for activator ions which can emit light upon excitation of the phosphor. Among these, transition metal Mn^{2+} is a good candidate due to its low cost and earth abundant nature. Unlike rare earth ions that have multiple characteristic emission peaks, Mn^{2+} ions exhibit tunable and single band emission [12,13]. Now, when choosing a host matrix for activator incorporation, it is ensured that they are either wide band gap semiconductors with bandgap greater than 2.8 eV or insulating materials with a much higher band gap. This is to make sure that the activator energy levels are introduced into the band gap of the host. Secondly, the operational temperatures of an LED can range upto 85^{o}C-150 ^{o}C and hence the thermal stability and resistance to water ingress must also be considered when selecting the appropriate phosphor hosts [14,15]. In addition, the activator's access to an homovalent doping site in the host along with the crystal field associated with it are also to be considered. For a long time, oxide hosts have been employed for this purpose in view of their high thermal and ambient stability. Often, the oxide compounds are formed in non-stoichiometric forms due to the deoxygenation that occurs at high synthesis temperatures as a result of unintentional defects [16–18]. Eventhough, in some cases defect related luminescence is said to be a bane turned into a boon, it is not the same in all cases and a precise control over the lattice imperfections are necessary. This can be done using passivation techniques which will then increase the production costs and introduce other complexities. Hence, it is imperative to find a host with high defect tolerance so that its optoelectronic (emission) properties are not affected by the presence of defects.

In this aspect, halide perovskites can be an excellent choice for a luminescent host matrix since it possess the necessary high defect tolerance as the dominant defects in these materials introduce only shallow levels which generally does not trap carriers [19]. Thus, the introduced shallow levels does not affect the band structure and preserve the material properties unlike deep traps. Another interesting aspect of halide

perovskites is that they can be prepared through facile solution processing techniques despite its vulnerability of producing greater crystal imperfections [19]. This aspect is not because of low density of defects in halide perovskites but due to their defect tolerant nature. In the last 10 years, perovskite halides have displayed excellent photophysical properties and prospective potential for various optoelectronic devices. Perovskite halides have ABX_3 stoichiometry and its structure is made up of alternative corner shared octahedra's that extends in all the three directions with the A site cations located in the cuboctahedral cavities formed by these octahedra's. The B site is usually occupied by divalent cations with ns^2 configurations such as Pb^{2+} or Ge^{2+} and the A-site is an organic amine or an alkali metal cation and the X sites are halides viz I, Br, Cl.

Despite the fact that research on perovskite halides has been going on for quite some time, the recent surge in their studies are due to their application as a photovoltaic absorber material by Kojima et al in 2009 with a power conversion efficiency (PCE) of 3.9% [20]. Subsequent researches have improved the PCE from 3.9% to 25.7 % and is now comparable to the performance of Si solar cells. In case of emission properties, all inorganic perovskite halides in particular have achieved near unity photoluminescent quantum yield (PLQY) with tunable wavelength across the entire visible spectrum by tuning the halide composition [21]. Organometallic perovskite quantum dots also exhibit 100% PLQY due to its exciton confinement [22]. The narrow emission band in these materials satisfies the requirements of large color gamut demanding devices such as displays, photodetectors, lasers and scintillators. In addition to defect tolerance and bandgap, exciton binding energy has a significant effect on the optical properties of materials. An exciton is defined as a coupling of electron and hole in a mutual columbic interaction forming a quasi-neutral particle. For luminescent applications, higher exciton binding energies are required for better radiative recombination. This has been achieved in perovskite halides by nanostructuring to have dimensional physical barriers for exciton dissociation.

Perovskites halides can be broadly classified into two categories based on its constituents, one is the "organic-inorganic/hybrid" perovskite halides and the other is the "All inorganic" perovskite halides. As mentioned earlier the first report of 3.9 % PCE in solar cells was based on $MAPbI_3$ (MA = Methylammonium) belongs to this family of hybrid perovskites. Though the hybrid perovskites exhibit magnificent properties, they are bounded by its instability and toxicity. For instance, the best

performing $MAPbI_3$ degrades into methylamine and Iodine gas along with a yellow lead iodide residue on exposure to heat, moisture and UV light. These thermal and moisture instability of $MAPbI_3$ arises from the organic part of the perovskite ‘methylamine” which has the acidic hydrogen atoms and these are responsible for their instability. As a consequence, organic cations without acidic hydrogen atoms have to be substituted at the 'A' site to remove this instability. Some examples of acidic hydrogen free organic ammonium cations include tetraethylammonium and tetramethylammonium cations. Yet another route is to incorporate inorganic 'Cs' atoms at the 'A' site to completely eliminate this instability and maintaining its excellent properties. There are still other limitations to these perovskite halides apart from its instability.

Inspite of its outstanding characteristics, the presence of toxic lead in the structure limits its upscaling and use in real time devices. On that account, it is essential to develop materials that maintain the three dimensional structural integrity of the perovskite halides and also retain its exceptional properties without the presence of lead (Pb^{2+}) in the structure. One way to solve this is to replace two Pb^{2+} ions in ABX_3 perovskite halides by one trivalent and one monovalent cations simultaneously which give rise to the double perovskite composition $A_2B'B''X_6$ (A=Cs^+, Rb^+, B'=Na^+, Ag^+, B''=Bi^{3+}, In^{3+}, Sb^{3+}, Cr^{3+}, X=Br, Cl). These compounds came to the limelight with the discovery of alike absorption properties in $Cs_2AgBiBr_6$ with that of the organic-inorganic perovskite $MAPbBr_3$ in the year 2016.

Double perovskites have drawn a lot of attention as potential lead-free materials due to their excellent stability against heat, moisture and light. Double perovskites have similar structural features in comparison with the perovskite halides but the difference exists at the octahedral arrangement. In the molecular sense, the adjacent corner shared octahedra’s in double perovskites are made of different cations of B’ and B’’. The double perovskite halides can be prepared in different ways for various optoelectronic applications such as thin films, nanocrystals and single crystals. Perovskite halides have many advantages over other phosphor host systems such as oxides due to their easy compositional flexibility and solution processability at temperatures near 100 ^oC. Mostly, the respective hydrohalic acids are used as solvents and the precipitation takes place without any additional agents. The capacity to dope ions with different ionic radius and oxidation states gives more degree of freedom to develop double perovskites that can be used as light emitters.

2. Literature survey

Liu et al. [23] reported the optical properties of Mn^{2+} doped Cs_2PbX_3 nanocrystals synthesized using combined hot injection and anion exchange route. They observed a strong orange - yellow emissions at 586 nm with a PLQY of 27 % from Mn^{2+} : $CsPbCl_3$ nanocrystals with 9.6 atomic % of Mn^{2+} substitution at the Pb site. Zhang et al. [24] successfully doped Mn^{2+} in 0-D perovskite Cs_4PbCl_6 using modified hot injection synthesis at 180 ^oC. Here, the replacement of Pb^{2+} by Mn^{2+} led to highly intense luminescence at 607 nm with a PLQY of 25.8 % along with an ultralong decay time of 26 ms. This enhanced emission is attributed to the high exciton binding energy in Mn^{2+}:Cs_4PbCl_6 perovskites owing to the presence of isolated $PbCl_6$ octahedras and enhanced energy transfer to Mn^{2+} ions. Xu et al.[25] demonstrated a core – isostructural shell passivation strategy to intensify the luminescence in Mn^{2+}:$CsPbCl_3$ nanocrystals. Apart from passivation, this strategy was also used to internalize the Mn^{2+} ions to the nanocrystals center where the exciton wavefunction amplitude is higher and results in improved energy transfer to Mn^{2+} ions and higher PLQY. The $CsPbCl_3$ outer shell passivated Mn^{2+}:$CsPbCl_3$ nanocrystals shows a broader orange emission at 600 nm with a FWHM of 100 nm and a PLQY of 39 %. But, almost all of Mn^{2+} : $CsPbCl_3$ quantum dots have an excitation wavelength that is restricted to the ultraviolet (UV) to violet region. However, phosphors in most commercial white LED's are driven by blue emitting InGaN chips. Hence it is necessary to extend the excitation wavelength from UV to blue region.

Chen et al. [26] demonstrated this by tuning the bandgap of $CsPbCl_3$ by an anion exchange of Cl with Br and prepared visible light (blue) excitable Mn^{2+}:$CsPb(Cl/Br)_3$@SiO_2 quantum dots with an orange luminescence at 600 nm with a PLQY of 30 %. Here, the role of SiO_2 coating is to increase the ambient stability and to decrease the loss of Mn^{2+} from the quantum dots which arises due to the large ionic radii mismatch between the Pb^{2+} and Mn^{2+} ions. Biswas et al. [27] reported Mn^{2+} doping in 2D layered perovskite $(C_4H_9NH_3)_2PbBr_4$ synthesized using a combined slow cooling and ball milling approach with a wide orange emission peaked at 600 nm with a PLQY of 39% and an FWHM of 80 nm. The better luminescence performance of this system was due to the increased transfer of energy from the tightly bound excitons of the layered perovskites to the Mn^{2+} energy levels. Sumit et al.[28] reported solution processed single crystalline Mn^{2+} : $(C_4H_{12}N)_2PbBr_4$ layered perovskites with dazzling

orange emission at 600 nm with a PLQY of 61 % and a lifetime of 0.67 ms. In addition, these perovskite halides also exhibited rigorous stability under thermal treatment at a temperature of 200^{o}C in ambient atmosphere for over 24 hours [28]. Zhou et al.[29] reported Mn^{2+} doping in 2D organic-inorganic perovskite $(C_4H_9NH_3)_2PbCl_4$ using mechanochemical synthesis route indicating facile incorporation of Mn^{2+} through simple diffusion in the $(C_4H_9NH_3)_2PbCl_4$ perovskite. This results in an emission at 615 nm along with a PLQY of 27%. Biwu ma et al. [30] reported Mn^{2+} : $(C_6H_{18}N_2O_2)PbBr_4$ single component white light emitting phosphor with an emission range across the entire visible spectrum (400-700 nm) and a PLQY of 28 %. The strong white emission is the result of the synergistic effect of the red emission from Mn^{2+} and blue luminescence from the trapped excitons of $(C_6H_{18}N_2O_2)PbBr_4$ perovskite. Zhou et al. [31] successfully prepared lead free $Cs_2AgInCl_6$ single crystals by hydrothermal method with an optical bandgap of 3.23 eV and a defect induced broad red luminescence at 635 nm under an excitation of 370 nm. Volanakis et al.[32] reported $Cs_2AgInCl_6$ using precipitation method with an emission peak at 608 nm (FWHM =120 nm) attributed to the defect related transitions. Wang et al.[33] reported double doping of Bi^{3+} and Ce^{3+} to improve the photophysical properties of $Cs_2AgInCl_6$ nanocrystals. This design approach was used to passivate the surface dangling bonds of chloride ions along with a reduction of silver vacancies which enhances the PLQY from 10 to 26 % and blueshifts the emission peak from 591 to 580 nm resulting in an orange emission. This luminescence originates from the radiative recombination of self- trapped excitons.

Wei et al. [34] reported self-trapped exciton induced orange luminescence in Ce^{3+}, Bi^{3+} : $Cs_2Ag_{0.4}Na_{0.6}InCl_6$ at 570 nm with an efficiency of 98.6% and an FWHM of 156 nm. Nie et al.[35] demonstrated tunable blue to red luminescence on Ho^{3+} doping in Sb^{3+}: $Cs_2NaInCl_6$ double perovskites at an UV excitation of 318 nm. The PLQY of the narrow red luminescence from Ho^{3+} ions increased gradually from 0 to 72 % on increasing the Ho^{3+} concentration from 0 to 21.5%, while the PLQY of blue self-trapped exciton luminescence from the $SbCl_6$ octahedra was nearly quenched from 99 % to 0 on increasing the Ho^{3+} content. This signifies the existence of an effective energy transfer pathway from the blue emitting $SbCl_6$ octahedras to the red active Ho^{3+} centers. They also demonstrated a good PLQY of 51.2 % on shifting the excitation wavelength from 318 to 450 nm for their integration with commercial blue emitting LED chips.

From the literature review, it was identified that, most Mn^{2+} doped lead chloride systems are toxic and their best emitting nanostructures such as colloidal quantum dots and nanocrystals are unstable and tend to agglomerate which results in the decrease of their red luminescence performance. Thus, from review's analysis and the concept was conceived to produce Mn^{2+} doped $A_2B'B''X_6$ double perovskite systems, which could be expected to have red emissions and various concentrations, have been planned.

3. Objective

The objectives of this thesis are as follows,

- Synthesis of lead free octahedral shaped Mn^{2+} doped A2B'B''X_6 double perovskite systems such as $Cs_2NaBiCl_6$, $Cs_2AgBiCl_6$, $Cs_2AgInCl_6$ and $Cs_2NaInCl_6$ microcrystals using chemical reflux method.
- The synthesized Mn^{2+} doped double perovskites have been characterized using different analytical techniques such as X-ray diffraction (XRD), Raman spectroscopy, Energy dispersive X-ray and X-ray photoelectron spectroscopies to understand their structural, vibrational properties and also confirm their composition. The morphologies of the double perovskites were studied using scanning electron microscopy.
- The thermal stability of double perovskite phosphors have been analyzed using TGA and DTA analysis.
- Rietveld analysis of the XRD spectra of all pure and Mn^{2+} doped double perovskites have been carried out to understand the microstructural changes in the lattice upon doping such as variation in the lattice parameters, unit cell volume and metal - halide bond length changes.
- Electron density analysis of Mn^{2+} doped double perovskites have been performed to deduce the substitutional sites of Mn^{2+} in the double perovskite lattice and also to understand the evolution of metal-halide bonding characteristics upon Mn^{2+} doping.
- Finally, the optical investigations have been done using UV-visible, and photoluminescence (PL) spectroscopies to understand the optical absorption and light emission behavior of the double perovskites. Time correlated single photon counting measurements of the respective emissions have been carried out to understand the decay dynamics and charge carrier relaxation of these transitions.

4. Research problem

As the primary needs of an optically pumped white light emitting diode is to have an efficient warm white emission with high color rendering index (CRI) and correlated color temperature (CCT). However, most commercial LEDs have a deficiency of red emission which is the cause of low CRI and CCT. Lead free double perovskites have not been widely studied as phosphor hosts even though it possess high stability and similar optoelectronic properties to lead halide perovskites. The potential red emitting Mn^{2+} doped lead halide phosphors are limited by low stability, toxicity and poor emission efficiency. Transition metal-based red emitting phosphors have been taken into consideration in place of the conventionally thought of rare earth activators that included inorganic phosphors. Due to the abundance of Mn, this makes OP-LEDs less expensive. As a result, increasing Mn^{2+} red phosphor sources should increase the relative percentage of red emission. It has been intended to create the Mn^{2+} doped $A_2B'B''X_6$ double perovskite systems, which may be anticipated to have red emissions. The effect of varied concentrations on the Mn^{2+} systems on the double perovskites could be studied for OP-LED applications. Hence, to resolve these limitations, Mn^{2+} doped lead-free double perovskite phosphors has been presented.

In this aspect, we have studied various environmentally friendly Mn^{2+} doped double perovskite phosphors with efficient red emission and high thermal stability such as $Cs_2NaBiCl_6$, $Cs_2AgBiCl_6$, $Cs_2AgInCl_6$ and $Cs_2NaInCl_6$.Also, the cost of the host systems is reduced by using a straight forward chemical reflux method, and the complex analysis of luminescence performance with an emphasis on PL intensity have been taken as a research challenge and researched. Overall, this thesis focuses on addressing the toxicity, instability of lead halide perovskites by introducing double perovskites and enhancing the weakly luminescing double perovskites by Mn^{2+} doping. The schematic of the chemical reflux method used to prepare Mn^{2+}: $Cs_2B'B''Cl_6$ (B'= Na^+, Ag^+, B''= Bi^{3+}, In^{3+}) double perovskites are shown in Figure 1. In a typical synthesis, 10 ml of hydrochloric acid (37%) was taken in a two necked round bottom flask. To this solution stoichiometric amounts of B' (Na^+, Ag^+) and B'' (Bi^{3+}, In^{3+}) metal chloride salts were added and heated at 105^{o}C for 2 hours with simultaneous magnetic stirring. Then twice the ratio of anhydrous cesium chloride was added which immediately results in the formation of $Cs_2B'B''Cl_6$ precipitate. The solution is heated at the same temperature for 1 more hour for complete reaction of the precursors. Then, the obtained precipitate was

washed with ethanol for three times and dried in the hot air oven at 95°C. For the synthesis of Mn^{2+} doped double perovskites, 0.08 mmol (0.0158 g), 0.17mmol (0.0336 g), 0.34 mmol (0.0672 g), 0.68 mmol (0.1345 g) of manganese chloride tetrahydrate was added before the addition of cesium chloride in respective solutions. The nominal Mn^{2+} doping ratio is calculated using the formula: (Mn/B'+B"). These samples are denoted by CB'B"C 0.08, CB'B"C 0.17, CB'B"C 0.34, and CB'B"C 0.68 unless specified otherwise. When adding Mn^{2+}, amount of other starting materials was kept same as that of pure one. The product formation is described by equations (1) and (2),

$$2CsCl + B'Cl + B''Cl_3 \rightarrow Cs_2B'B''Cl_6 \quad (1)$$

$$2CsCl + (2x)\ MnCl_2 + (1-x)\ Na'Cl + (1-x)Bi''Cl_3 \rightarrow Cs_2B'_{(1-x)}B''_{(1-x)}Mn_{(2x)}Cl_6 \quad (2)$$

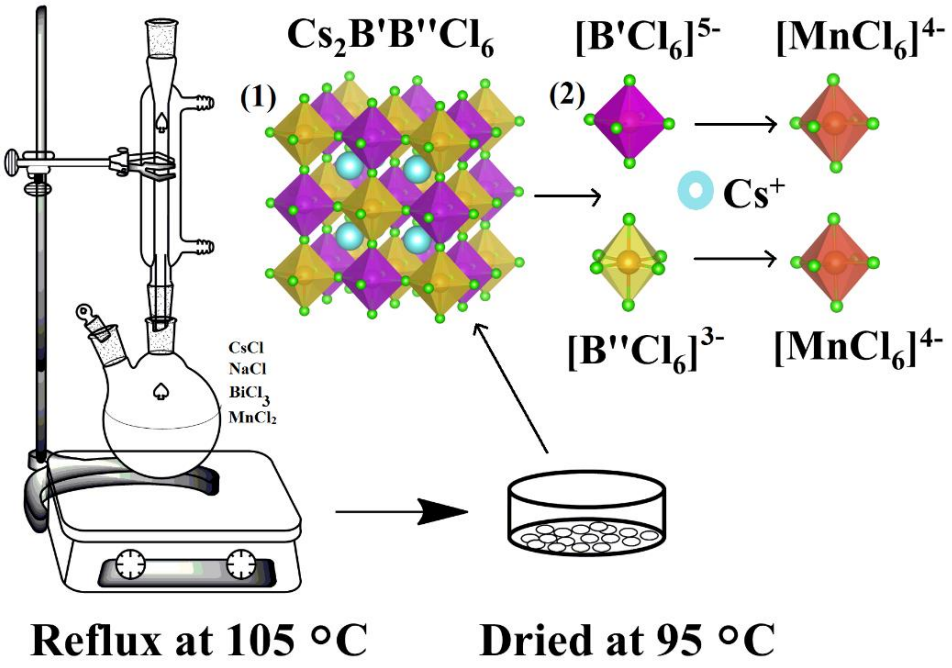

Figure 1 Pictorial representation of Mn^{2+}: $Cs_2B'B''Cl_6$ microcrystal preparation by chemical reflux method. Inset (1) shows the crystal structure of pure $Cs_2B'B''Cl_6$ and (2) depicts the replacement of $[B'Cl_6]^{5-}$ and $[B''Cl_6]^{3-}$ by $[MnCl_6]^{4-}$ octahedra.

5. Organization of thesis

The above research problem is shown as a flowchart in Figure 2. The work presented in this thesis show preparation and characterization of various lead free Mn^{2+}

doped red emitting phosphors with good thermal stability and high PL intensity. Besides the luminescence investigations, their structural, vibrational, bonding and absorption properties are also analyzed. The contents of the planned thesis are as follows:

Chapter 1 discusses the background of lighting and the need for reducing the energy demand of light sources. It also enlists the role of LED and phosphor materials in energy saving lighting and the operating principles of an LED. A detailed introduction into types of luminescence, design of a phosphor material, charge transfer mechanisms and the importance of perovskite halides are discussed.

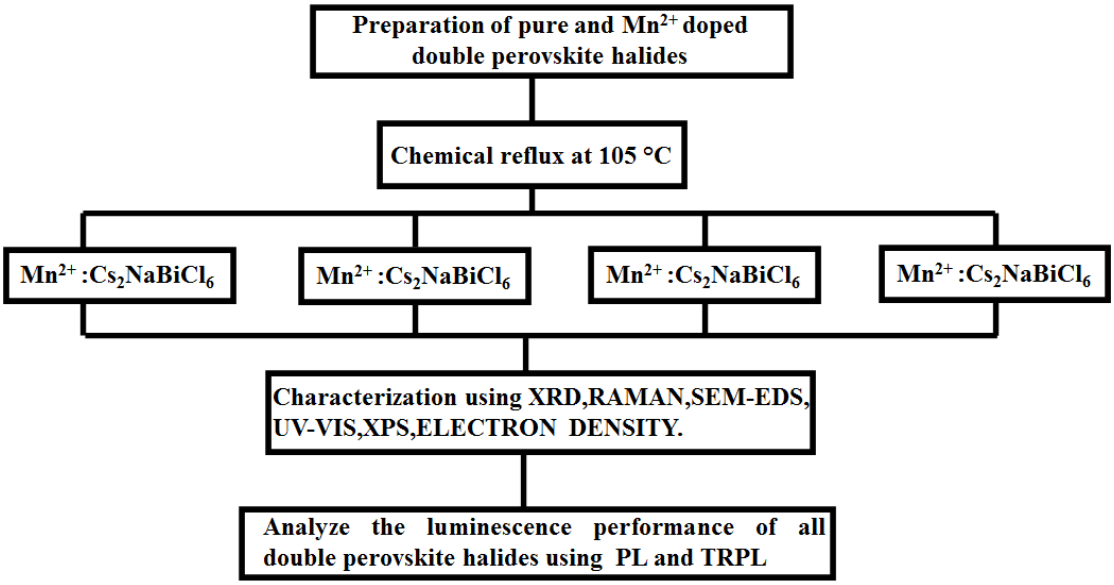
Preparation of pure and Mn2+ doped double perovskite halides
Chemical reflux at 105 °C
Mn2+ :Cs2NaBiCl6
Mn2+ :Cs2NaBiCl6
Mn2+ :Cs2NaBiCl6
Mn2+ :Cs2NaBiCl6
Characterization using XRD,RAMAN,SEM-EDS, UV-VIS,XPS,ELECTRON DENSITY.
Analyze the luminescence performance of all double perovskite halides using PL and TRPL

Figure 2 Overview of the research process carried out.

Chapter 2 describes the survey of literature covering the present work and the advances in lead halide perovskite phosphors. The perovskite and double perovskite halides doped with transition metals (Mn^{2+}) are extensively studied as light emitting phosphors due to the tunable emission range of their d-d transition. Based on the literature review, a research gap have been identified and lead free double perovskites have been identified as the suitable host material for light emitting phosphors. The scope of the thesis work has been presented at the end of this chapter along with the thesis outline.

Chapter 3 outlines the precursors used for the synthesis of lead free double perovskites and transition metal Mn^{2+} doped double perovskites. Besides, various characterization techniques used for analyzing the structural phase, morphology, vibrational modes, and optical properties are explained in detail along with their instrumentation and principle of operation.

Chapter 4 deals about the preparation and characterization of solution processed Mn^{2+}: $Cs_2NaBiCl_6$ microcrystals. Mn^{2+}: $Cs_2NaBiCl_6$ double perovskites crystallize in cubic symmetry for all Mn^{2+} feed ratios. The crystallanity increases with increase in Mn^{2+} concentration due to ordering of the Na^+ and Bi^{3+} cations. Rietveld refinement of the XRD spectra revealed the decrease of Bi-Cl bond length and the lattice constant on Mn^{2+} doping. The decrease in Bi-Cl bond lengths observed in refinement were also corroborated by Raman spectral studies which evinced a shift of all Raman modes to higher energies on Mn^{2+} doping. SEM analysis revealed that well defined octahedral morphologies were obtained on Mn^{2+} incorporation. The percentage of Mn^{2+} incorporation are identified by using EDS studies. Electron density investigations reveal the evolution of Bi-Cl bonds from a strong ionic character to a strong covalent character on Mn^{2+} doping indicating the substitutional replacement of Bi^{3+} by the Mn^{2+} ions. Indirect bandgaps calculated using Tauc plot were found to decrease from 3.49 to 3.46 eV on Mn^{2+} doping. Mn^{2+}:$Cs_2NaBiCl_6$ double perovskites exhibited orange-red luminescence at 585 nm at an excitation of 354 nm. Long lifetime of 11 ms for the 585 nm emission obtained time resolved photoluminescence analysis also verify that luminescence is indeed from Mn^{2+} spin forbidden transitions. Thus, the observed hybridization of Bi 4f and Cl 2p orbitals leads to increased carrier transport within $BiCl_6$ octahedra for improved energy transfer to Mn^{2+} ions and results in efficient orange - red luminescence in Mn^{2+} doped $Cs_2NaBiCl_6$ double perovskites.

Chapter 5 discusses the chemical reflux synthesis of Mn^{2+}: $Cs_2AgBiCl_6$ double perovskites and its luminescence performance. XRD analysis confirm that $Fm\bar{3}m$ symmetry with a cubic structure remains invariant for all Mn^{2+} : $Cs_2AgBiCl_6$. Refinement results indicated a decrease in lattice constant and volume of unit cell upon Mn^{2+} doping. Further, refinement also evinces decrease in both Ag-Cl and Bi-Cl bond lengths on increasing Mn^{2+} feed ratios in $Cs_2AgBiCl_6$. Shift of Raman vibrational modes to higher frequencies also validates this observation. Homogeneous octahedral

morphologies with near uniform size distributions were observed for Mn^{2+} doped $Cs_2AgBiCl_6$ double perovskites. One dimensional charge density distributions of Mn^{2+}: $Cs_2AgBiCl_6$ clearly demonstrates the Mn^{2+} substitution at both Ag^+ and Bi^{3+} sites. Band gaps determined from Tauc plot varied from 2.65 to 2.69 eV on Mn^{2+} doping. Mn^{2+} incorporation in $Cs_2AgBiCl_6$ resulted in a red emission at 601 nm on exciting with a 420 nm light and this emission is ascribed to the $^4T_1$-$^6A_1$ transition of Mn^{2+} ions. The emission intensity increased with increasing the Mn^{2+} concentration and it reached maximum for 0.9 at % of Mn^{2+}. An average decay time of 0.34 ms determined for the 601 nm emission further substantiates the spin forbidden Mn^{2+} relaxation pathway for the electrons.

Chapter 6 describes the preparation of Mn^{2+} : $Cs_2AgInCl_6$ using reflux route. XRD revealed that no morphotrophic phase transitions occurred for Mn^{2+} doping in $Cs_2AgInCl_6$ and the crystallite size increased with increase in Mn^{2+} concentration. Rietveld refinements disclosed the decrease in unit cell volume, lattice constant and Ag-Cl bond lengths upon Mn^{2+} doping. Increase in energy of optical phonon modes observed from the Raman studies on Mn^{2+} incorporation also authenticate the refinement results. Octahedral morphology was observed for the 0.6 % Mn^{2+} doped $Cs_2AgInCl_6$.Variation in mid bond electron densities for the Ag-Cl and In-Cl bonds indicated the replacement of both Ag^+/$In3^+$ by Mn^{2+} ions. Direct band gap of $Cs_2AgInCl_6$ was tuned from 3.42 to 3.60 eV on Mn^{2+} doping. A red luminescence at 616 nm was observed from PL studies at an UV excitation of 340 nm and are assigned to the radiative relaxations of electrons from $^4T_1$ to $^6A_1$ states of Mn^{2+} ions. Overlap of the PL excitation spectra with the absorption spectra indicates that the Mn^{2+} ions are sensitized by the $Cs_2AgInCl_6$ host. Time resolved PL spectra indicated a long lifetime of 0.83 ms for the 616 nm emission which further certify the spin forbidden origin of the 616 nm emission.

Chapter 7 deals about the Mn^{2+} incorporation in $Cs_2NaInCl_6$ double perovskites. XRD studies evince cubic structure for all Mn^{2+}: $Cs_2NaInCl_6$. XRD refinements disclose the decrease of In-Cl, Na-Cl bonds along with a decrease in the lattice and unit cell volume of Mn^{2+} doping. This decrease in bond lengths is further substantiated by the blue shift of the Raman modes for all Mn^{2+}: $Cs_2NaInCl_6$. SEM dark field imaging manifested octahedral shaped particles for Mn^{2+}: $Cs_2NaInCl_6$. 2-D and 1-D electron

density investigations evince the substitution of Mn^{2+} at both In^{3+} and Na^{+} sites. Large increase in the absorption of $Cs_2NaInCl_6$ is due to the relaxation of parity forbidden transitions upon Mn^{2+} doping. Direct bandgaps were found to increase from 4.02 for pure $Cs_2NaInCl_6$ to 4.12 eV on Mn^{2+} doping. Near UV excitable (320 nm) red emission was observed at 614 nm corresponding to the d-d transition of Mn^{2+} ions. This Mn^{2+} origin of emission is further endorsed by a long life time of 2.1 ms as obtained from time resolved PL measurements.

Chapter 8 of the thesis presents the overall summary and conclusions of all research work investigated. It also outline the ways to enhance the present research and also scope for future directions in this research field. The summary demonstrates that the Mn^{2+} doped double perovskite halide phosphors are non-toxic, environment friendly, possess high heat stability and exhibit good red luminescence performance for optically pumped white LED's. Intriguingly, all four phosphors systems thermal stability range from 502 – 616 ^{o}C and thus can be used in high power flood lighting LED's. We believe that this research will pave a new inroad into the development and design of stable lead free double perovskite phosphors for lighting applications.

REFERENCES

[1] B. Stoffel, The Role of Pumps for Energy Consumption and Energy Saving, in: Assess. Energy Effic. Pumps Pump Units, Elsevier, (2015), 1–24.

[2] C.-F. Chen, LEDs for liquid crystal display (LCD) backlighting, in: Nitride Semicond. Light. Diodes, Elsevier, (2018), 619–646.

[3] M. Worku, L.J. Xu, M. Chaaban, A. Ben-Akacha, B. Ma, Optically pumped white light-emitting diodes based on metal halide perovskites and perovskite-related materials, *APL Materials*, **8** (1) (2020), 010902.

[4] Y. Kawano, S.W. Kim, T. Ishigaki, K. Uematsu, K. Toda, H. Takaba, M. Sato, Site engineering concept of Ce^{3+}-activated novel orange-red emission oxide phosphors, *Optical Materials Express*, **4** (9) (2014), 1770.

[5] G. Li, Y. Tian, Y. Zhao, J. Lin, Recent progress in luminescence tuning of Ce^{3+} and Eu^{2+}-activated phosphors for pc-WLEDs, *Chemical Society Reviews*, **44** (23) (2015), 8688–8713.

[6] J. Zhong, D. Chen, Y. Zhou, Z. Wan, M. Ding, W. Bai, Z. Ji, New Eu^{3+} -activated perovskite $La_{0.5}Na_{0.5}TiO_3$ phosphors in glass for warm white light emitting diodes, *Dalton Transactions*, **45** (11) (2016), 4762–4770.

[7] B. Qiao, S. Zhao, Z. Xu, X. Xu, Synthesis of ZnO quantum dots and their agglomeration mechanisms along with emission spectra based on ageing time and temperature, *Chinese Physics B*, **25** (9) (2016), 098102.

[8] Z. Xie, Z. Yin, Y. Wu, C. Liu, X. Hao, Q. Du, X. Xu, White Light-Emitting Diodes Based on Individual Polymerized Carbon Nanodots, *Scientific Reports*, **7** (1) (2017), 12146.

[9] D. Dupont, M.D. Tessier, P.F. Smet, Z. Hens, Indium Phosphide-Based Quantum Dots with Shell-Enhanced Absorption for Luminescent Down-Conversion, *Advanced Materials*, **29** (29) (2017), 1700686.

[10] C. Ruan, X. Bai, C. Sun, H. Chen, C. Wu, X. Chen, H. Chen, V.L. Colvin, W.W. Yu, White light-emitting diodes of high color rendering index with polymer dot phosphors, *RSC Advances*, **6** (108) (2016), 106225–106229.

[11] F. Li, C. Nie, L. You, X. Jin, Q. Zhang, Y. Qin, F. Zhao, Y. Song, Z. Chen, Q. Li, White light emitting device based on single-phase CdS quantum dots, *Nanotechnology*, **29** (20) (2018), 205701.

[12] S. S, S. D, S. V, Y. Li, R. Ramanathan, I. S, Three dimensional atomistic-scale electron density distribution analysis of $ZnWO_4$: Sm phosphors, *Optik*, **249** (September 2021) (2022), 168169.

[13] Y. Zhang, J.D. Lin, V. Vijayaragavan, K.K. Bhakoo, T.T.Y. Tan, Tuning sub-10 nm single-phase $NaMnF_3$ nanocrystals as ultrasensitive hosts for pure intense fluorescence and excellent T1 magnetic resonance imaging, *Chemical Communications*, **48** (83) (2012), 10322.

[14] A. Różowicz, H. Wachta, K. Baran, M. Leśko, S. Różowicz, Arrangement of LEDs and Their Impact on Thermal Operating Conditions in High-Power Luminaires, *Energies*, **15** (21) (2022), 8142.

[15] R. A., R.K. C., C. V.P., Experimental analysis on estimating junction temperature and service life of high power LED array, *Microelectronics Reliability*, **120** (May) (2021), 114121.

[16] P. Mondal, Effect of Oxygen vacancy induced defect on the optical emission and excitonic lifetime of intrinsic ZnO, *Optical Materials*, **98** (December) (2019), 109476.

[17] J. Zhang, J. Shi, D.-C. Qi, L. Chen, K.H.L. Zhang, Recent progress on the electronic structure, defect, and doping properties of Ga_2O_3, *APL Materials*, **8** (2) (2020), 020906.

[18] J. Cooke, P. Ranga, J. Jesenovec, J.S. McCloy, S. Krishnamoorthy, M.A. Scarpulla, B. Sensale-Rodriguez, Effect of extended defects on photoluminescence of gallium oxide and aluminum gallium oxide epitaxial films, *Scientific Reports*, **12** (1) (2022), 3243.

[19] J. Kang, L.W. Wang, High Defect Tolerance in Lead Halide Perovskite $CsPbBr_3$, *Journal of Physical Chemistry Letters*, **8** (2) (2017), 489–493.

[20] A. Kojima, K. Teshima, Y. Shirai, T. Miyasaka, Organometal halide perovskites as visible-light sensitizers for photovoltaic cells, *Journal of the American Chemical Society*, **131** (17) (2009), 6050–6051.

[21] L. Protesescu, S. Yakunin, M.I. Bodnarchuk, F. Krieg, R. Caputo, C.H. Hendon, R.X. Yang, A. Walsh, M. V. Kovalenko, Nanocrystals of Cesium Lead Halide Perovskites ($CsPbX_3$, X = Cl, Br, and I): Novel Optoelectronic Materials Showing Bright Emission with Wide Color Gamut, *Nano Letters*, **15** (6) (2015), 3692–3696.

[22] S.-W. Dai, B.-W. Hsu, C.-Y. Chen, C.-A. Lee, H.-Y. Liu, H.-F. Wang, Y.-C. Huang, T.-L. Wu, A. Manikandan, R.-M. Ho, C.-S. Tsao, C.-H. Cheng, Y.-L. Chueh, H.-W. Lin, Perovskite Quantum Dots with Near Unity Solution and Neat-Film Photoluminescent Quantum Yield by Novel Spray Synthesis, *Advanced Materials*, **30** (7) (2018), 1705532.

[23] W. Liu, Q. Lin, H. Li, K. Wu, I. Robel, J.M. Pietryga, V.I. Klimov, Mn^{2+} -Doped Lead Halide Perovskite Nanocrystals with Dual-Color Emission Controlled by Halide Content, *Journal of the American Chemical Society*, **138** (45) (2016), 14954–14961.

[24] W. Zhang, J. Wei, Z. Gong, P. Huang, J. Xu, R. Li, S. Yu, X. Cheng, W. Zheng, X. Chen, Unveiling the Excited-State Dynamics of Mn^{2+} in 0D Cs_4 $PbCl_6$ Perovskite Nanocrystals, *Advanced Science*, **7** (22) (2020), 2002210.

[25] K. Xu, C.C. Lin, X. Xie, A. Meijerink, Efficient and Stable Luminescence from Mn^{2+} in Core and Core–Isocrystalline Shell $CsPbCl_3$ Perovskite Nanocrystals, *Chemistry of Materials*, **29** (10) (2017), 4265–4272.

[26] D. Chen, G. Fang, X. Chen, Silica-Coated Mn-Doped $CsPb(Cl/Br)_3$ Inorganic Perovskite Quantum Dots: Exciton-to-Mn Energy Transfer and Blue-Excitable Solid-State Lighting, *ACS Applied Materials & Interfaces*, **9** (46) (2017), 40477–40487.

[27] A. Biswas, R. Bakthavatsalam, J. Kundu, Efficient Exciton to Dopant Energy Transfer in Mn^{2+} -Doped $(C_4H_9NH_3)_2PbBr_4$ Two-Dimensional (2D) Layered Perovskites, *Chemistry of Materials*, **29** (18) (2017), 7816–7825.

[28] S.K. Dutta, A. Dutta, S. Das Adhikari, N. Pradhan, Doping Mn^{2+} in Single-Crystalline Layered Perovskite Microcrystals, *ACS Energy Letters*, **4** (1) (2019), 343–351.

[29] G. Zhou, S. Guo, J. Zhao, M. Molokeev, Q. Liu, J. Zhang, Z. Xia, Unraveling the mechanochemical synthesis and luminescence in MnII-based two-dimensional hybrid perovskite $(C_4H_9NH_3)_2PbCl_4$, *Science China Materials*, **62** (7) (2019), 1013–1022.

[30] C. Zhou, Y. Tian, O. Khabou, M. Worku, Y. Zhou, J. Hurley, H. Lin, B. Ma, Manganese-Doped One-Dimensional Organic Lead Bromide Perovskites with Bright White Emissions, *ACS Applied Materials & Interfaces*, **9** (46) (2017), 40446–40451.

[31] J. Zhou, Z. Xia, M.S. Molokeev, X. Zhang, D. Peng, Q. Liu, Composition design, optical gap and stability investigations of lead-free halide double perovskite $Cs_2AgInCl_6$, *Journal of Materials Chemistry A*, **5** (29) (2017), 15031–15037.

[32] G. Volonakis, A.A. Haghighirad, R.L. Milot, W.H. Sio, M.R. Filip, B. Wenger, M.B. Johnston, L.M. Herz, H.J. Snaith, F. Giustino, $Cs_2InAgCl_6$: A New Lead-Free Halide Double Perovskite with Direct Band Gap, *The Journal of Physical Chemistry Letters*, **8** (4) (2017), 772–778.

[33] S. Wang, J. Qi, S. V. Kershaw, A.L. Rogach, Co-Doping of Cerium and Bismuth into Lead-Free Double Perovskite $Cs_2AgInCl_6$ Nanocrystals Results in Improved Photoluminescence Efficiency, *ACS Nanoscience Au*, **2** (2) (2022), 93–101.

[34] C.-Y. Wang, P. Liang, R.-J. Xie, Y. Yao, P. Liu, Y. Yang, J. Hu, L. Shao, X.W. Sun, F. Kang, G. Wei, Highly Efficient Lead-Free (Bi,Ce)-Codoped $Cs_2Ag_{0.4}Na_{0.6}InCl_6$ Double Perovskites for White Light-Emitting Diodes, *Chemistry of Materials*, **32** (18) (2020), 7814–7821.

[35] J. Nie, H. Li, S. Fang, B. Zhou, Z. Liu, F. Chen, Y. Wang, Y. Shi, Efficient red photoluminescence in holmium-doped $Cs_2NaInCl_6$ double perovskite, *Cell Reports Physical Science*, **3** (4) (2022), 100820.

LIST OF PUBLICATIONS

[1] M. Jeevaraj, S. Sudhahar, P. Devendran, N. Nallamuthu, N.D. Jayram, M.K. Kumar, Structural, optical and charge density investigations on lead free Mn^{2+} doped $Cs_2NaBiCl_6$ double perovskite microcrystals, *Materials Today Communications*, **33** (October) (2022), 104715.

[2] M. Jeevaraj, P. Devendran, N. Nallamuthu, S. Sudhahar, M.K. Kumar, Influence of Mn^{2+} doping on the optical properties of $Cs_2AgBiCl_6$ double perovskite luminescent phosphors, *Journal of Materials Science: Materials in Electronics*, **34** (1) (2023), 65.

[3] M. Jeevaraj, S. Sudhahar, N. Nallamuthu, P. Devendran, S. Saravanakumar, D. Sivaganesh, M.K. Kumar, Solution processed Mn^{2+} doped $Cs_2AgInCl_6$ lead free double perovskite as a potential light emitting material, *Physica B: Condensed Matter*, **653** (January) (2023), 414679.

[4] M. Jeevaraj, P Devendran, N. Nallamuthu, S. Sivaganesh, S. Saravanakumar, S. Asath Bahadur, M. Krishna Kumar, Extrinsic electronic states to tune the luminescence and bonding nature of $Cs_2NaInCl_6$ double perovskite. (Under Communication in Journal of Alloys and Compounds).